

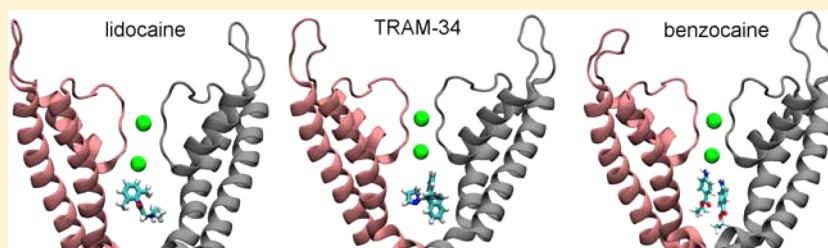
# Mechanisms and Energetics of Potassium Channel Block by Local Anesthetics and Antifungal Agents

Rong Chen,<sup>\*,†</sup> Ganna Gryn'ova,<sup>‡</sup> Yingliang Wu,<sup>§</sup> Michelle L. Coote,<sup>‡</sup> and Shin-Ho Chung<sup>†</sup>

<sup>†</sup>Research School of Biology and <sup>‡</sup>Research School of Chemistry, Australian National University, Canberra, ACT 0200, Australia

<sup>§</sup>College of Life Sciences, Wuhan University, Wuhan, China

## S Supporting Information



**ABSTRACT:** Many drug molecules inhibit the conduction of several families of cation channels by binding to a small cavity just below the selectivity filter of the channel protein. The exact mechanisms governing drug–channel binding and the subsequent inhibition of conduction are not well understood. Here the inhibition of two  $K^+$  channel isoforms, Kv1.2 and  $K_{Ca}3.1$ , by two drug molecules, lidocaine and TRAM-34, is examined in atomic detail using molecular dynamics simulations. A conserved valine-alanine-valine motif in the inner cavity is found to be crucial for drug binding in both channels, consistent with previous studies of similar systems. Potential of mean force calculations show that lidocaine in its charged form creates an energy barrier of  $\sim 6 kT$  for a permeating  $K^+$  ion when the ion is crossing over the drug, while the neutral form of lidocaine has no significant effect on the energetics of ion permeation. On the other hand, TRAM-34 in the neutral form is able to create a large energy barrier of  $\sim 10 kT$  by causing the permeating ion to dehydrate. Our results suggest that TRAM-34 analogues that remain neutral and permeable to membranes under acidic conditions common to inflammation may act as possible drug scaffolds for combating local anesthetic failure in inflammation.

Many small drug molecules and short peptides are known to inhibit the conduction of biological ion channels, which are important therapeutic targets for certain diseases. The ionic pathway of several families of cation channels such as  $K^+$  and  $Na^+$  channels comprises three segments: a narrow selectivity filter, an inner cavity, and a hydrophobic conduit leading to the intracellular space. Some polypeptides isolated from animal venoms inhibit cation channels by binding to the outer vestibular wall while inserting the side chain of a lysine residue into the selectivity filter.<sup>1,2</sup> In contrast, small drug molecules such as local anesthetics and antifungal agents (e.g., clotrimazole) permeate through the cell membrane and enter the inner cavity of ion channels through the intracellular gate.<sup>3,4</sup> The inner cavity is a common receptor site for a variety of drugs,<sup>4</sup> highlighting its pharmacological significance.

Clotrimazole is a potent inhibitor of the  $Ca^{2+}$ -activated  $K^+$  channel of intermediate conductance,  $K_{Ca}3.1$ ,<sup>5</sup> which is a promising target for immunosuppressant agents.<sup>6,7</sup> However, clotrimazole also potently inhibits the cytochrome P450 reductase, a membrane-bound enzyme.<sup>8</sup> Analogues of clotrimazole with a reduced affinity for P450 reductase have been developed as drug candidates for the treatment of autoimmune diseases.<sup>9</sup> Substitution of the imidazole ring in clotrimazole required for P450 inhibition with a pyrazole ring leads to the

analogue TRAM-34 (Figure 1A), which inhibits  $K_{Ca}3.1$  potently ( $K_d = 20$  nM) but is ineffective for certain isoforms of P450 enzymes.<sup>9,10</sup> Thus, the potential to develop novel antifungal and immunosuppressant agents from clotrimazole analogues is enormous.

The receptor sites of both clotrimazole and TRAM-34 in  $K_{Ca}3.1$  are in the inner cavity. A charged and membrane-impermeable analogue of clotrimazole is effective in blocking  $K_{Ca}3.1$  only when introduced into the cytoplasm,<sup>11,12</sup> suggesting that the receptor site is accessible from the intracellular side. Clotrimazole thus is believed to permeate through the membrane and act on the inner cavity of the channel upon being applied from the extracellular side.<sup>11</sup> This mechanism resembles that of local anesthetics, which primarily act on  $Na^+$  channels but also inhibit  $K^+$  and  $Ca^{2+}$  channels by binding to the inner cavity.<sup>3</sup> Both clotrimazole and local anesthetics are small molecules carrying one or more aromatic rings, which confer the solubility of the drugs in lipids required for the drugs to penetrate through cell membranes. However, a notable difference is that clotrimazole is predominantly neutral

Received: July 30, 2014

Revised: September 16, 2014

Published: October 9, 2014



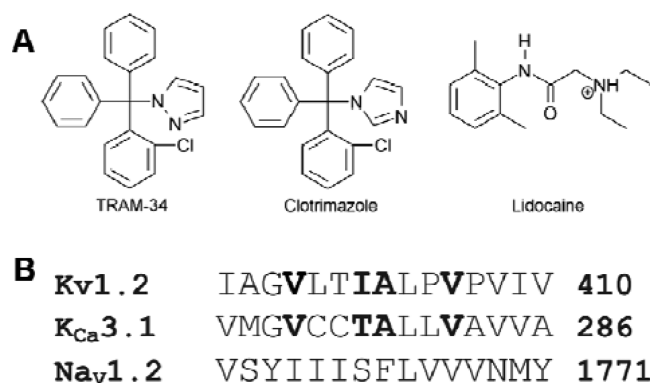


**Figure 1.** (A) Chemical structures of TRAM-34, clotrimazole, and lidocaine showing their expected protonation states at biological pH. The calculated  $pK_a$  values of their conjugate bases are 0.64, 6.01, and 10.08, respectively (*vide infra*). (B) Sequence alignment of Kv1.2, K<sub>Ca</sub>3.1, and Na<sub>v</sub>1.2 in the inner cavity region near the intracellular gate. Key residues in Na<sub>v</sub>1.2 likely to be involved in local anesthetic binding (ref 49) are underlined.

while lidocaine carries a positive charge at a neutral pH (Figure 1A). The positive charge of lidocaine is believed to be important for its inhibitory action on ion channels through electrostatic repulsion to permeating cations.<sup>13</sup> The question of how TRAM-34 and other neutral drug molecules would inhibit ion channel conduction arises. The modes of binding of various neutral molecules to the inner cavity of K<sup>+</sup> and Na<sup>+</sup> channels have been examined extensively using computational methods.<sup>14–17</sup> These studies have provided insights into the possible interactions involved in drug–channel binding, but the link between drug binding and subsequent channel inhibition remains to be fully established. For example, the drug can either physically occlude the conduction pathway of an open channel<sup>18</sup> or stabilize the channel in a nonconducting state.<sup>19–21</sup> Understanding how the energetics of ion permeation is altered by drug binding would help discriminate between alternative mechanisms of action.

Here the mechanism by which lidocaine and TRAM-34 inhibit two potassium channels, Kv1.2 and K<sub>Ca</sub>3.1, in the open state is examined using molecular dynamics (MD) simulations with explicit solvents. The key residues in Kv1.2 and K<sub>Ca</sub>3.1 that are responsible for the binding of the two drug molecules are identified, and the effect of drug binding on the energetics of ion permeation is derived. Lidocaine binds to the inner cavity of Kv1.2 with a micromolar affinity and must be charged to inhibit the conduction of the open channel. In contrast, the presence of one neutral TRAM-34 molecule is sufficient to inhibit conduction by creating a large energy barrier for permeating ions that have to shed one or two water molecules in its hydration shell to move through the inner cavity that is partially occluded by the drug. These results have broad implications for the development of drugs targeting the inner cavity of ion channels.

## METHODS

**Molecular Dynamics Simulations.** Structures of Kv1.2 and K<sub>Ca</sub>3.1 in the open state embedded in 1-palmitoyl-2-oleoyl-*sn*-glycero-3-phosphocholine lipid bilayers were taken from previous studies.<sup>22,23</sup> While several crystal structures of the bacterial Ca<sup>2+</sup>-activated K<sup>+</sup> channel MthK are available, the sequence similarity between MthK and K<sub>Ca</sub>3.1 is poor especially in the S6 region, which is important for drug binding (Figure

S1A of the Supporting Information). The structure of K<sub>Ca</sub>3.1 is modeled on the crystal structure of Kv1.2 in the open state, which is highly structurally similar with MthK (Figure S1B of the Supporting Information). With this homology model of K<sub>Ca</sub>3.1, we have accurately reproduced the current–voltage relationship of the channel, and the binding affinities of two scorpion toxins for the channel have been determined experimentally.<sup>23</sup> Lidocaine and TRAM-34 are placed in the inner cavity of the channels. The resulting systems are then equilibrated for 30 ns each without restraints, allowing the drug molecules to evolve to the most favorable position and orientation in the binding site.

All MD simulations are performed under periodic boundary conditions using NAMD 2.9.<sup>24</sup> The CHARMM36 force fields for lipids<sup>25</sup> and proteins<sup>26</sup> and the TIP3P model for water<sup>27</sup> are used. Topologies of benzocaine, lidocaine, and TRAM-34 are generated using the ParamChem server (<https://www.paramchem.org>).<sup>28,29</sup> The penalty score is less than 50 for 90% of atoms and less than 10 for 60% of atoms of lidocaine and TRAM-34, and less than 10 for all the atoms of benzocaine, indicating that the analogy between the drugs and existing molecules in the force field is reasonable. The CHARMM general force field is used to describe the drug molecules.<sup>30</sup> The switch and cutoff distances for short-range interactions are set to 8.0 and 12.0 Å, respectively. Using the particle mesh Ewald method with a maximal grid spacing of 1.0 Å accounts for the long-range electrostatic interactions. Bond lengths are maintained rigid with the SHAKE<sup>31</sup> and SETTLE<sup>32</sup> algorithms. A time step of 2 fs is used. The temperature and pressure are maintained constant at 300 K on average by using the Langevin dynamics (damping coefficient of 1 ps<sup>−1</sup>) and 1 atm on average by using the Nosé–Hoover Langevin Piston method.<sup>33</sup> The barostat oscillation and damping time scales are set to 200 and 100 ps, respectively. The pressure coupling is semiisotropic. Trajectories are saved every 20 ps for analysis.

**Umbrella Sampling.** The potential of mean force (PMF) profiles for the binding of drug molecules and a permeating K<sup>+</sup> ion to the inner cavity of Kv1.2 and K<sub>Ca</sub>3.1 are constructed using the umbrella sampling method. The  $K_d$  values for drug binding are derived according to the following equation:<sup>34,35</sup>

$$K_d^{-1} = 1000\pi R^2 N_A \int_{z_{\min}}^{z_{\max}} \exp[-W(z)/kT] dz \quad (1)$$

where  $R$  is the radius of the cylinder (5 Å),  $N_A$  is Avogadro's number,  $z_{\min}$  and  $z_{\max}$  are the boundaries of the binding site along the channel axis ( $z$ ), and  $W(z)$  is the PMF.

The starting structures of the umbrella windows spaced at 0.5 Å intervals are generated by moving the drug molecule or ion along the reaction coordinate ( $z$ ) followed by energy minimization. The biasing potential of each umbrella window is 30 kcal mol<sup>−1</sup> Å<sup>−2</sup>. The center of mass (COM) of the channel backbone is at  $z = 0$  Å. A flat-bottom harmonic restraint is applied to maintain the COM of the drug or ion within a cylinder with a radius of 5 Å centered on the channel axis. The radius of the cylinder ensures that the restraining potential is always zero when the drug or ion is inside the channel. Each umbrella window is simulated for at least 5 ns to ensure good convergence. The first 1 ns of each window is removed from data analysis. The  $z$  coordinate of the toxin COM is saved every picosecond for analysis.

**Quantum-Chemical Calculations.** Standard *ab initio* and density functional theory calculations have been performed using Gaussian 09<sup>36</sup> and Molpro 2012.1.<sup>37</sup> Accurate gas-phase

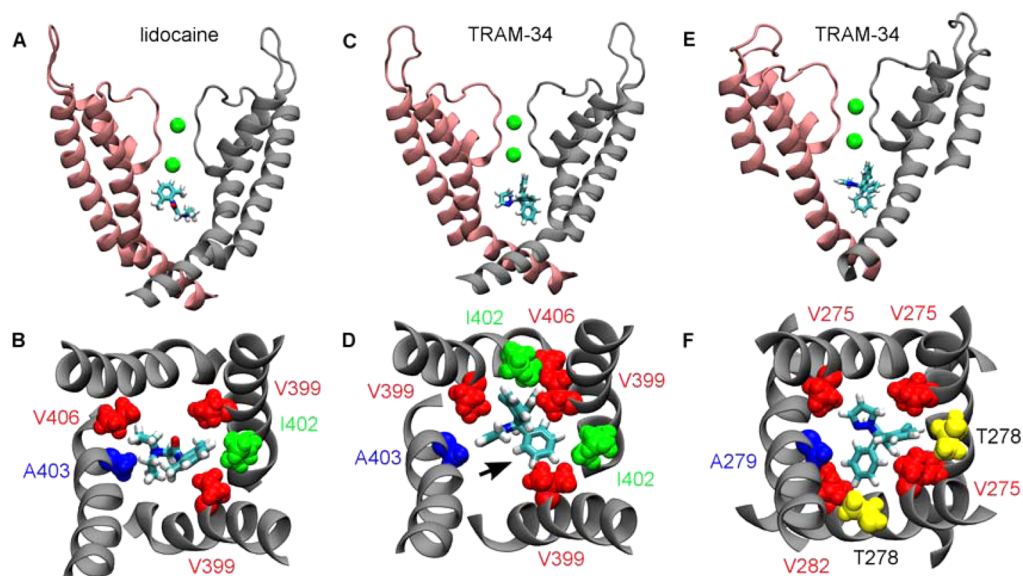


**Figure 2.** Modes of binding of lidocaine and TRAM-34 to Kv1.2 (A–D) and TRAM-34 to  $K_{Ca}3.1$  (E and F). Two of the four subunits of the channels (shown as pink and gray ribbons), viewed perpendicular to the channel axis, together with two  $K^+$  ions (green) in the selectivity filter, and the drug molecules in the inner cavity are displayed in the top row (A, C, and E). The positions of lidocaine and TRAM-34 relative to the inner cavity of the channels are shown in the bottom row (B, D, and F). All four subunits forming the inner cavity are viewed here from periplasmic side of the channel axis. The positions of key hydrophobic residues lining the cavity are indicated. In panel D, the arrow indicates the least rigid benzene ring.

Gibbs free energies of all species at 25 °C were calculated using the G3(MP2,CC)(+) method<sup>38</sup> in conjunction with M06-2X<sup>39</sup>/6-31+G(d) geometries and frequencies and corrected for the effects of aqueous solvation using the UAKS-CPCM/B3LYP/6-31+G(d) method.<sup>40</sup>  $pK_a$  values were calculated using the proton exchange method. These procedures were previously shown to reproduce experimental data within chemical accuracy.<sup>41–43</sup> A complete description of the computational procedures can be found in the Supporting Information.

## RESULTS AND DISCUSSION

**Binding of Lidocaine to Kv1.2.** Local anesthetics block  $K^+$  channels effectively at clinically relevant concentrations, although the analgesic effect of these drugs is primarily due to their inhibition of  $Na^+$  channels involved in pain pathways.<sup>44,45</sup> The selectivity of lidocaine for  $Na^+$  channels over  $K^+$  channels is only  $\sim 5$ -fold.<sup>44</sup> To understand the general principles governing the inhibition of cation channels by local anesthetics, the binding of lidocaine to the crystal structure of Kv1.2 in the open state<sup>46,47</sup> is examined using MD simulations.

Figure 2A shows the position of lidocaine relative to the selectivity filter of Kv1.2 after 30 ns of an unbiased MD simulation. A benzene ring of the drug is in the proximity of the  $K^+$  ion at the S4 site of the filter. The distance between the ion and the COM of the benzene ring is  $6 \pm 1$  Å, and the ion lies at an oblique angle to the benzene ring, indicating that the cation– $\pi$  interactions are weak.<sup>48</sup> The drug molecule also interacts with a number of hydrophobic residues lining the inner cavity of the channel (Figure 2B). Residues Val399, Ile402, Ala403, and Val406, which correspond closely to the key residues of  $Na^+$  channels for etidocaine uncovered experimentally (Figure 1B),<sup>49</sup> are in close contact with the drug.

**Binding of TRAM-34 to Kv1.2 and  $K_{Ca}3.1$ .** In contrast to lidocaine, which is nonselective for a wide range of cation

channels, TRAM-34 is  $\sim 200$ -fold selective for  $K_{Ca}3.1$  over Kv1.2.<sup>6</sup> Understanding the selectivity mechanism of TRAM-34 may facilitate the design of specific drugs targeting the inner cavity of ion channels. With this aim in mind, we examine the modes of binding of TRAM-34 to Kv1.2 and  $K_{Ca}3.1$ .

Figure 2C shows the position of TRAM-34 relative to the selectivity filter of Kv1.2 after an equilibrium simulation of 30 ns. Unlike lidocaine, whose benzene ring forms weak cation– $\pi$  interactions with a filter ion, TRAM-34 is not observed to interact significantly with the  $K^+$  ion at the S4 site of the filter. The distance between the  $K^+$  ion and the COM of the nearest benzene ring in TRAM-34 is  $7 \pm 1$  Å. The drug is also surrounded by a hydrophobic ring formed by the side chains of residues Val399, Ile402, Ala403, and Val406 (Figure 2D).

The position of TRAM-34 in the inner cavity of  $K_{Ca}3.1$ , also predicted from an unbiased simulation of 30 ns, is shown in Figure 2E. The mode of binding of TRAM-34 to  $K_{Ca}3.1$  is similar to that of TRAM-34 to Kv1.2. The heterocyclic moiety of TRAM-34 does not protrude into the filter of the channel. The key residues in  $K_{Ca}3.1$  involved in the binding of TRAM-34 include V275, Thr278, Ala279, and V282, which form a VAV motif (Figure 2F), which is also found in the region of Kv1.2 involved in binding the drugs (Figure 2A–D). This is in agreement with previous studies in which an equivalent VAV motif was shown to be involved in the binding of various small molecules to Kv1.5.<sup>14,50</sup> In addition to the VAV motif, Thr250 at the inner end of the filter of  $K_{Ca}3.1$  also interacts intimately with TRAM-34 (Figure S2 of the Supporting Information), consistent with mutagenesis experiments in which the V275A and T250S mutations of  $K_{Ca}3.1$  reduced the affinity of TRAM-34 by more than 1000-fold.<sup>12</sup>

**Energetics of Drug Binding.** To understand the energetics of the binding of lidocaine and TRAM-34 to Kv1.2 and  $K_{Ca}3.1$  in the open state, we construct PMF profiles under various conditions. On the basis of the PMF profiles of drug–channel dissociation, it is possible to derive the dissociation

constant ( $K_d$ ) or half-maximal inhibitory concentration ( $IC_{50}$ ), which is measurable experimentally, using eq 1 derived previously.<sup>34,35</sup> The convergence of the PMF profiles is demonstrated in Figure S3 of the Supporting Information. The calculated  $K_d$  values closely mirror those determined experimentally, suggesting that the modes of binding between the drugs and channels predicted from MD simulations (Figure 2) are realistic.

Figure 3 shows that the well depth of the PMF profile for lidocaine-Kv1.2 is  $\sim 13$   $kT$ , corresponding to a  $K_d$  value of 20

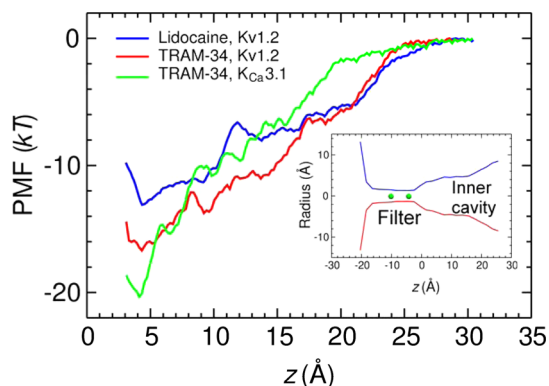


**Figure 3.** PMF profiles for the dissociation of lidocaine and TRAM-34 from Kv1.2 and  $K_{Ca3.1}$ . The inset shows the radius of the channel along the channel axis ( $z$ ). The positions of two filter ions are indicated with two green spheres.

$\mu M$ . Although the  $K_d$  value of lidocaine for Kv1.2 in the open state has not been determined experimentally, it is known that lidocaine inhibits  $K^+$  currents effectively at a concentration of 1 mM.<sup>44,45</sup> The  $K_d$  value of lidocaine for Kv1.3, whose primary structure is identical to that of Kv1.2 in the inner cavity region, has been estimated to be 0.6 mM,<sup>51</sup> which is only 30-fold lower than the value we predicted for Kv1.2. Thus, the  $K_d$  value we predicted is in broad agreement with experiment.

TRAM-34 is  $\sim 40$ -fold more potent than lidocaine in binding Kv1.2. The PMF profile of TRAM-34–Kv1.2 binding shows a well depth of 16.5  $kT$  (Figure 3), corresponding to a  $K_d$  value of 540 nM, within 1 order of magnitude to the value of 4.5  $\mu M$  determined experimentally.<sup>6</sup> The well depth of the profile for TRAM-34– $K_{Ca3.1}$  binding is 20.3  $kT$ , which would predict a  $K_d$  value of 10 nM, in the proximity of the experimental value of 20 nM.<sup>6</sup> To further verify models of TRAM-34 in complex with  $K_{Ca3.1}$ , we derive the PMF profiles for the binding of the drug to two mutant channels (T250S and V275A). The well depth of the PMF profiles for the mutant channels is 8–10  $kT$  shallower than that of the wide type (Figure S4 of the Supporting Information), indicating that the drug binds the mutant channels 3000–20000-fold weaker, in line with experiment.<sup>12</sup> Thus, the affinities of TRAM-34 for  $K_{Ca3.1}$  and Kv1.2 observed experimentally are reproduced.

**Mechanism of TRAM-34 Selectivity.** TRAM-34 is  $\sim 200$ -fold selective for  $K_{Ca3.1}$  over Kv1.2, as shown experimentally<sup>6</sup> and in our PMF calculations (Figure 3). The difference in the PMF profiles of binding of TRAM-34 to the two channels is partially due to TRAM-34 being more rigid on binding to  $K_{Ca3.1}$  than Kv1.2.

The motion of TRAM-34, when it is bound to the inner cavity of  $K_{Ca3.1}$ , is highly restricted. In contrast, it can tumble more freely in the binding cavity of Kv1.2. As shown in Figure

S5 of the Supporting Information, the root-mean-square fluctuation of the 25 heavy atoms of TRAM-34 ranges from 0.5 to 1.4  $\text{\AA}$ , substantially lower than the equivalent value obtained when it is bound to Kv1.2. Thus, the binding of TRAM-34 to  $K_{Ca3.1}$  leads to a greater entropic loss, which is offset by a more favorable enthalpy of binding.

The interaction between the drug and the channel is largely determined by the residues from the binding pocket in the inner cavity of the channels. The binding pocket of TRAM-34 contains a polar threonine at position 278 in  $K_{Ca3.1}$ , as opposed to an apolar isoleucine at the equivalent position (402) in Kv1.2. Thus, the pyrazole ring of TRAM-34 would interact more favorably with Thr278 of  $K_{Ca3.1}$  (interaction energy of  $-10.4 \pm 0.1$   $kT$ ) than with Ile402 of Kv1.2 (interaction energy of  $-6.4 \pm 0.1$   $kT$ ).

The binding of TRAM-34 also causes the inner cavity to be dehydrated in both channels. We define the  $C\alpha$  atoms of residues Kv1.2-Thr374 (or  $K_{Ca3.1}$ -Thr250) and Kv1.2-Val410 (or  $K_{Ca3.1}$ -Ala286) as the upper and lower boundary of the inner cavity and calculate the number of water molecules in this region over the last 10 ns of the simulation. In the absence of TRAM-34, approximately 39 water molecules ( $39 \pm 5$ ) are present in the cavity of Kv1.2. Once TRAM-34 is bound, however, this number is reduced to only  $28 \pm 3$ , suggesting that the binding of TRAM-34 causes the inner cavity of Kv1.2 to be dehydrated by 11 water molecules. Similarly, we find that 11 water molecules ( $37 \pm 3$  vs  $26 \pm 3$ ) are also ejected from the inner cavity of  $K_{Ca3.1}$  after the binding of TRAM-34.

**Role of Charge and Dehydration.** To investigate the effect of lidocaine and TRAM-34 on the energetics of ion permeation, we construct the PMF profile of a  $K^+$  ion as it permeates through the Kv1.2 channel from the intracellular side in the presence and absence of a drug molecule. We show that lidocaine in its charged form induces an energy barrier of approximately 6  $kT$  for a permeating  $K^+$  ion, consistent with a previous study.<sup>13</sup> However, the neutral form of lidocaine has no significant effect on the energetics of ion permeation. In contrast, the neutral TRAM-34 is able to create an energy barrier of  $\sim 10$   $kT$  by causing the permeating ion to dehydrate by more than one water molecule.

Figure 4A shows the PMF experienced by a  $K^+$  ion as it permeates from the intracellular gate to the inner cavity of Kv1.2, in the presence or absence of a drug molecule bound to the inner cavity. In the absence of a drug molecule, the energy barrier is  $\sim 2$   $kT$ . In the presence of lidocaine, the barrier increases to 8  $kT$ . Deprotonating lidocaine and removing the positive charge it carries reduce the energy barrier to only  $\sim 2$   $kT$ , comparable to the energy barrier in the absence of any drugs. This indicates that the positive charge carried by the terminal amine group of lidocaine is critical for the inhibitory effect of the drug.

TRAM-34 is even stronger than lidocaine in inhibiting the conduction of Kv1.2 despite its neutral charge and is observed to induce an energy barrier of more than 10  $kT$  for the permeating  $K^+$  ion (Figure 4A). This high energy barrier arises from the energy cost of dehydrating the ion when it attempts to pass around TRAM-34. Figure 4B shows the number of water molecules within the first hydration shell of the  $K^+$  ion as the ion is passing through the inner cavity of Kv1.2 occupied by lidocaine or TRAM-34. In the case of lidocaine, the number of water molecules in the hydration shell of the  $K^+$  ion remains constant along the reaction coordinate. In contrast, the hydration number of the ion is reduced from 4.8 to 3.4 when

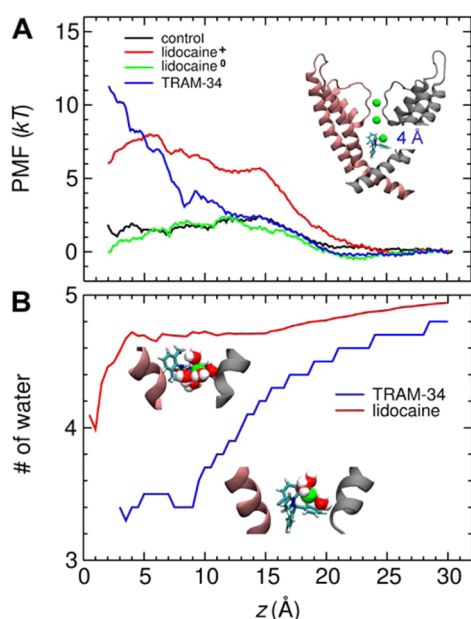


**Figure 4.** (A) PMF profiles of a permeating  $K^+$  ion along the channel axis of Kv1.2 in the absence (control) and presence of lidocaine and TRAM-34. In the inset, green spheres indicate the two  $K^+$  ions in the filter and the permeating ion. (B) Average number of water molecules within 3 Å of the permeating  $K^+$  ion (green sphere) as a function of the position of the ion along  $z$ .

the ion is crossing over TRAM-34, suggesting that the presence of TRAM-34 causes the permeating ion to be dehydrated by approximately 1.4 water molecules. This is consistent with the high energy barrier for the ion generated by TRAM-34 observed in PMF calculations (Figure 4A).

#### Implications for the Design of Novel Anesthetics.

Available local anesthetics consist of three principle components: an aromatic ring, an intermediate ester or amide linkage, and a terminal amine group.<sup>52</sup> The amine group generally has a  $pK_a$  of 7.6–8.9 and thus has a high probability of being protonated and hence charged at neutral pH. Without an amine group, the drug would be neutral and thus, according to the conventional charge-repulsion mechanism demonstrated previously and here for lidocaine, unable to inhibit ion channel conduction (Figure 4A). This would explain the fact that a terminal amine group is found in virtually all available local anesthetics, except for benzocaine, which in any case has a very low affinity ( $K_d = 1$  mM) for sodium channels.<sup>53,54</sup> However, our findings suggest that suitable neutral molecules, such as TRAM-34, can function as effective ion channel blockers by instead causing incoming ions to be dehydrated. In the case of benzocaine, which is smaller than TRAM-34, one molecule would not be able to cause ions to be dehydrated; however, multiple benzocaine molecules may act in concert.<sup>54</sup> Two or three benzocaine molecules readily occupy the inner cavity of Kv1.2 after 20 ns of an unbiased simulation (Figure 5). In both cases, the negatively charged nitrogen atom of the amine group of benzocaine is closely coupled with the  $K^+$  ion at the S4 site (average distance of 3.5 Å over the last 5 ns), thereby physically occluding the conduction pathway. Also, permeating ions would have to be dehydrated when crossing over benzocaine multimers. Employing the mechanism of TRAM-34 uncovered here, additional aliphatic and aromatic groups may be introduced into benzocaine to enhance its potency.

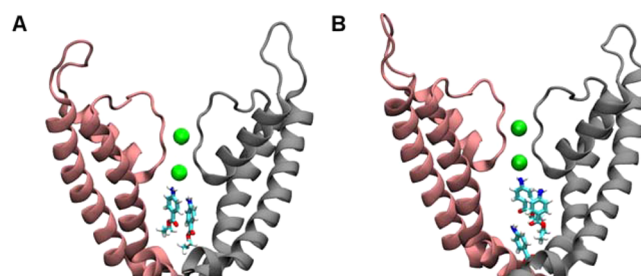


**Figure 5.** Positions of (A) two and (B) three benzocaine molecules relative to the inner cavity of Kv1.2 viewed perpendicular to the channel axis.

In further support of our mechanism, we note that, despite their terminal amine groups, a good proportion (10–40%) of local anesthetics are neutral at physiological pH.<sup>52</sup> The drug must move across the membrane in its neutral form and then become positively charged in the cytoplasm to block  $Na^+$  currents. Acidification can diminish local anesthetic potency,<sup>55</sup> possibly by reducing the number of drug molecules in the membrane-permeable neutral form. Thus, under certain conditions, such as inflammation, where the pH is acidic, the efficacy of local anesthetics can be compromised. A hypothesis for explaining this failure is that the drug becomes largely protonated and impermeable to cell membranes,<sup>56</sup> although other mechanisms may also be involved.<sup>57,58</sup> Our finding that suitably designed neutral molecules can act as effective ion channel blockers through a dehydration mechanism frees drug design from the necessity of designing local anesthetics that are positively charged. TRAM-34 analogues that are neutral and thus highly permeable to membranes at acidic pH may be designed. In Figure S6 of the Supporting Information, we show several examples of TRAM-34 analogues that, according to our calculations, are more resistant to protonation than classic local anesthetics such as lidocaine. These analogues are similar to the various TRAM-34 derivatives designed as connexin channel blockers previously.<sup>59</sup> TRAM-34 is known to inhibit sodium channel  $Na_v1.4$  potently with a  $K_d$  of 8  $\mu M$ .<sup>9</sup> By suitably tuning the polarity and size of the four rings that TRAM-34 carries, we might be able to design more specific and potent inhibitors for sodium channels involved in pain pathways as novel analgesics.

## CONCLUSIONS

In this work, the key molecular determinants and energetics of the binding of lidocaine and TRAM-34 to Kv1.2 and  $K_{Ca}3.1$  are examined in atomic detail using MD simulations with explicit solvents. In both channels in addition to a threonine at the inner end of the filter, a VAV motif in the inner cavity is involved in drug binding, consistent with previous studies performed on this drug molecule and other drug molecules.<sup>12,14,50</sup> Lidocaine must first cross the membrane deprotonated and then become protonated in the inner cavity to inhibit the ion conduction of a channel. On the other hand, TRAM-34 inhibits ion conduction effectively by forcing permeating ions to dehydrate and is thus effective in its neutral form. The advantage of this novel mode of blocking is that these drugs can be designed to remain effective under acidic conditions that are typical of inflammation. These results thus have broad implications for the development of drugs targeting the inner cavity of ion channels.

## ■ ASSOCIATED CONTENT

### ■ Supporting Information

Six figures and details of quantum-chemical calculations. This material is available free of charge via the Internet at <http://pubs.acs.org>.

## ■ AUTHOR INFORMATION

### Corresponding Author

\*E-mail: [rong.chen@anu.edu.au](mailto:rong.chen@anu.edu.au). Phone: +61-2-6125-4337. Fax: +61-2-6125-0739.

### Funding

This work was supported by the National Health and Medical Research Council of Australia and The Medical Advances Without Animals Trust (MAWA). M.L.C. gratefully acknowledges an ARC Future Fellowship.

### Notes

The authors declare no competing financial interest.

## ■ ACKNOWLEDGMENTS

This research was undertaken on the National Computational Infrastructure in Canberra, Australia, which is supported by the Australian Commonwealth Government.

## ■ REFERENCES

- (1) Yu, L., Sun, C., Song, D., Shen, J., Xu, N., Gunasekera, A., Hajduk, P. J., and Olejniczak, E. T. (2005) Nuclear magnetic resonance structural studies of a potassium channel-charybdotoxin complex. *Biochemistry* 44, 15834–15841.
- (2) Banerjee, A., Lee, A., Campbell, E., and Mackinnon, R. (2013) Structure of a pore-blocking toxin in complex with a eukaryotic voltage-dependent K<sup>+</sup> channel. *eLife* 2, e00594.
- (3) Scholz, A. (2002) Mechanisms of (local) anaesthetics on voltage-gated sodium and other ion channels. *Br. J. Anaesth.* 89, 52–61.
- (4) England, S., and de Groot, M. J. (2009) Subtype-selective targeting of voltage-gated sodium channels. *Br. J. Pharmacol.* 158, 1413–1425.
- (5) Ishii, T. M., Silvia, C., Hirschberg, B., Bond, C. T., Adelman, J. P., and Maylie, J. (1997) A human intermediate conductance calcium-activated potassium channel. *Proc. Natl. Acad. Sci. U.S.A.* 94, 11651–11656.
- (6) Bradding, P., and Wulff, H. (2009) The K<sup>+</sup> channels K<sub>Ca</sub>3.1 and Kv1.3 as novel targets for asthma therapy. *Br. J. Pharmacol.* 157, 1330–1339.
- (7) Wang, J., and Xiang, M. (2013) Targeting potassium channels Kv1.3 and K<sub>Ca</sub>3.1: Routes to selective immunomodulators in autoimmune disorder treatment? *Pharmacotherapy* 5, 515–528.
- (8) Rodrigues, A. D., Gibson, G. G., Ioannides, C., and Parke, D. V. (1987) Interactions of imidazole antifungal agents with purified cytochrome P-450 proteins. *Biochem. Pharmacol.* 36, 4277–4281.
- (9) Wulff, H., Miller, M. J., Hansel, W., Grissmer, S., Cahalan, M. D., and Chandy, K. G. (2000) Design of a potent and selective inhibitor of the intermediate-conductance Ca<sup>2+</sup>-activated K<sup>+</sup> channel, IKCa1: A potential immunosuppressant. *Proc. Natl. Acad. Sci. U.S.A.* 97, 8151–8156.
- (10) Agarwal, J. J., Zhu, Y., Zhang, Q. Y., Mongin, A. A., and Hough, L. B. (2013) TRAM-34, a putatively selective blocker of intermediate-conductance, calcium-activated potassium channels, inhibits cytochrome P450 activity. *PLoS One* 8, e63028.
- (11) Dunn, P. M. (1998) The action of blocking agents applied to the inner face of Ca<sup>2+</sup>-activated K<sup>+</sup> channels from human erythrocytes. *J. Membr. Biol.* 165, 133–143.
- (12) Wulff, H., Gutman, G. A., Cahalan, M. D., and Chandy, K. G. (2001) Delineation of the clotrimazole/TRAM-34 binding site on the intermediate conductance calcium-activated potassium channel, IKCa1. *J. Biol. Chem.* 276, 32040–32045.
- (13) McNulty, M. M., Edgerton, G. B., Shah, R. D., Hanck, D. A., Fozzard, H. A., and Lipkind, G. M. (2007) Charge at the lidocaine binding site residue Phe-1759 affects permeation in human cardiac voltage-gated sodium channels. *J. Physiol.* 581, 741–755.
- (14) Andér, M., Luzhkov, V. B., and Åqvist, J. (2008) Ligand binding to the voltage-gated Kv1.5 potassium channel in the open state: Docking and computer simulations of a homology model. *Biophys. J.* 94, 820–831.
- (15) Zhorov, B. S., and Tikhonov, D. B. (2013) Ligand action on sodium, potassium, and calcium channels: Role of permeant ions. *Trends Pharmacol. Sci.* 34, 154–161.
- (16) Wulff, H., and Zhorov, B. S. (2008) K<sup>+</sup> channel modulators for the treatment of neurological disorders and autoimmune diseases. *Chem. Rev.* 108, 1744–1773.
- (17) Bruhova, I., and Zhorov, B. S. (2007) Monte Carlo-energy minimization of correolide in the Kv1.3 channel: Possible role of potassium ion in ligand-receptor interactions. *BMC Struct. Biol.* 7, 5.
- (18) Tikhonov, D. B., and Zhorov, B. S. (2005) Sodium channel activators: Model of binding inside the pore and a possible mechanism of action. *FEBS Lett.* 579, 4207–4212.
- (19) Marzian, S., Stansfeld, P. J., Rapedius, M., Rinne, S., Nematian-Ardestani, E., Abbruzzese, J. L., Steinmeyer, K., Sansom, M. S., Sanguinetti, M. C., Baukrowitz, T., and Decher, N. (2013) Side pockets provide the basis for a new mechanism of Kv channel-specific inhibition. *Nat. Chem. Biol.* 9, 507–513.
- (20) Baukrowitz, T., and Yellen, G. (1996) Two functionally distinct subsites for the binding of internal blockers to the pore of voltage-activated K<sup>+</sup> channels. *Proc. Natl. Acad. Sci. U.S.A.* 93, 13357–13361.
- (21) Nau, C., and Wang, G. K. (2004) Interactions of local anesthetics with voltage-gated Na<sup>+</sup> channels. *J. Membr. Biol.* 201, 1–8.
- (22) Chen, R., and Chung, S. H. (2012) Structural basis of the selective block of Kv1.2 by maurotoxin from computer simulations. *PLoS One* 7, e47253.
- (23) Chen, R., and Chung, S. H. (2013) Molecular dynamics simulations of scorpion toxin recognition by the Ca<sup>2+</sup>-activated potassium channel K<sub>Ca</sub>3.1. *Biophys. J.* 105, 1829–1837.
- (24) Phillips, J. C., Braun, R., Wang, W., Gumbart, J., Tajkhorshid, E., Villa, E., Chipot, C., Skeel, R. D., Kalé, L., and Schulten, K. (2005) Scalable molecular dynamics with NAMD. *J. Comput. Chem.* 26, 1781–1802.
- (25) Klauda, J. B., Venable, R. M., Freites, J. A., O'Connor, J. W., Tobias, D. J., Mondragon-Ramirez, C., Vorobyov, I., MacKerell, A. D., Jr., and Pastor, R. W. (2010) Update of the CHARMM all-atom additive force field for lipids: Validation on six lipid types. *J. Phys. Chem. B* 114, 7830–7843.
- (26) MacKerell, A. D., Bashford, D., Bellott, M., Dunbrack, R. L., Evanseck, J. D., Field, M. J., Fischer, S., Gao, J., Guo, H., Ha, S., Joseph-McCarthy, D., Kuchnir, L., Kuczera, K., Lau, F. T. K., Mattos, C., Michnick, S., Ngo, T., Nguyen, D. T., Prodhom, B., Reiher, W. E., Roux, B., Schlenkrich, M., Smith, J. C., Stote, R., Straub, J., Watanabe, M., Wiórkiewicz-Kuczera, J., Yin, D., and Karplus, M. (1998) All-atom empirical potential for molecular modeling and dynamics studies of proteins. *J. Phys. Chem. B* 102, 3586–3616.
- (27) Jorgensen, W. L., Chandrasekhar, J., Madura, J. D., Impey, R. W., and Klein, M. L. (1982) Comparison of simple potential functions for simulating liquid water. *J. Chem. Phys.* 79, 926–935.
- (28) Vanommeslaeghe, K., and MacKerell, A. D., Jr. (2012) Automation of the CHARMM General Force Field (CGenFF) I: Bond perception and atom typing. *J. Chem. Inf. Model.* 52, 3144–3154.
- (29) Vanommeslaeghe, K., Raman, E. P., and MacKerell, A. D., Jr. (2012) Automation of the CHARMM General Force Field (CGenFF) II: Assignment of bonded parameters and partial atomic charges. *J. Chem. Inf. Model.* 52, 3155–3168.
- (30) Vanommeslaeghe, K., Hatcher, E., Acharya, C., Kundu, S., Zhong, S., Shim, J., Darian, E., Guvench, O., Lopes, P., Vorobyov, I., and Mackerell, A. D., Jr. (2010) CHARMM general force field: A force field for drug-like molecules compatible with the CHARMM all-atom additive biological force fields. *J. Comput. Chem.* 31, 671–690.

- (31) Ryckaert, J. P., Ciccotti, G., and Berendsen, H. J. C. (1977) Numerical integration of the cartesian equations of motion of a system with constraints: Molecular dynamics of *n*-alkanes. *J. Comput. Phys.* 23, 327–341.
- (32) Miyamoto, S., and Kollman, P. A. (1992) SETTLE: An analytical version of the SHAKE and RATTLE algorithm for rigid water models. *J. Comput. Chem.* 13, 952–962.
- (33) Martyna, G. J., Tobias, D. J., and Klein, M. L. (1994) Constant pressure molecular dynamics algorithms. *J. Chem. Phys.* 101, 4177–4189.
- (34) Allen, T. W., Andersen, O. S., and Roux, B. (2004) Energetics of ion conduction through the gramicidin channel. *Proc. Natl. Acad. Sci. U.S.A.* 101, 117–122.
- (35) Gordon, D., Chen, R., and Chung, S. H. (2013) Computational methods of studying the binding of toxins from venomous animals to biological ion channels: Theory and applications. *Physiol. Rev.* 93, 767–802.
- (36) Frisch, M. J., Trucks, G. W., Schlegel, H. B., Scuseria, G. E., Robb, M. A., Cheeseman, J. R., Scalmani, G., Barone, V., Mennucci, B., Petersson, G. A., Nakatsuji, H., Caricato, M., Li, X., Hratchian, H. P., Izmaylov, A. F., Bloino, J., Zheng, G., Sonnenberg, J. L., Hada, M., Ehara, M., Toyota, K., Fukuda, R., Hasegawa, J., Ishida, M., Nakajima, T., Honda, Y., Kitao, O., Nakai, H., Vreven, T., Montgomery, J. A., Jr., Peralta, J. E., Ogliaro, F., Bearpark, M. J., Heyd, J., Brothers, E. N., Kudin, K. N., Staroverov, V. N., Kobayashi, R., Normand, J., Raghavachari, K., Rendell, A. P., Burant, J. C., Iyengar, S. S., Tomasi, J., Cossi, M., Rega, N., Millam, N. J., Klene, M., Knox, J. E., Cross, J. B., Bakken, V., Adamo, C., Jaramillo, J., Gomperts, R., Stratmann, R. E., Yazyev, O., Austin, A. J., Cammi, R., Pomelli, C., Ochterski, J. W., Martin, R. L., Morokuma, K., Zakrzewski, V. G., Voth, G. A., Salvador, P., Dannenberg, J. J., Dapprich, S., Daniels, A. D., Farkas, Ö., Foresman, J. B., Ortiz, J. V., Cioslowski, J., and Fox, D. J. (2009) *Gaussian 09*, Gaussian, Inc., Wallingford, CT.
- (37) Werner, H. J., Knowles, P. J., Knizia, G., Manby, F. R., and Schütz, M. (2012) Molpro: A general-purpose quantum chemistry program package. *Comput. Mol. Sci.* 2, 242–253.
- (38) Curtiss, L. A., Raghavachari, K., Redfern, P. C., Baboul, A. G., and Pople, J. A. (1999) Gaussian-3 theory using coupled cluster energies. *Chem. Phys. Lett.* 314, 101–107.
- (39) Zhao, Y., and Truhlar, D. G. (2008) The M06 suite of density functionals for main group thermochemistry, thermochemical kinetics, noncovalent interactions, excited states, and transition elements: Two new functionals and systematic testing of four M06-class functionals and 12 other functionals. *Theor. Chem. Acc.* 120, 215–241.
- (40) Tomasi, J., Mennucci, B., and Cammi, R. (2005) Quantum mechanical continuum solvation models. *Chem. Rev.* 105, 2999–3093.
- (41) Gryn'ova, G., Marshall, D. L., Blanksby, S. J., and Coote, M. L. (2013) Switching radical stability by pH-induced orbital conversion. *Nat. Chem.* 5, 474–481.
- (42) Ho, J., and Coote, M. L. (2009) pKa Calculation of some biologically important carbon acids: An assessment of contemporary theoretical procedures. *J. Chem. Theory Comput.* 5, 295–306.
- (43) Ho, J., and Coote, M. L. (2010) A universal approach for continuum solvent pKa calculations: Are we there yet? *Theor. Chem. Acc.* 125, 3–21.
- (44) Bräu, M. E., Vogel, W., and Hempelmann, G. (1998) Fundamental properties of local anesthetics: Half-maximal blocking concentrations for tonic block of Na<sup>+</sup> and K<sup>+</sup> channels in peripheral nerve. *Anesth. Analg. (Hagerstown, MD, U.S.)* 87, 885–889.
- (45) Komai, H., and McDowell, T. S. (2001) Local anesthetic inhibition of voltage-activated potassium currents in rat dorsal root ganglion neurons. *Anesthesiology* 94, 1089–1095.
- (46) Chen, X., Wang, Q., Ni, F., and Ma, J. (2010) Structure of the full-length Shaker potassium channel Kv1.2 by normal-mode-based X-ray crystallographic refinement. *Proc. Natl. Acad. Sci. U.S.A.* 107, 11352–11357.
- (47) Long, S. B., Campbell, E. B., and Mackinnon, R. (2005) Voltage sensor of Kv1.2: Structural basis of electromechanical coupling. *Science* 309, 903–908.
- (48) Gallivan, J. P., and Dougherty, D. A. (1999) Cation- $\pi$  interactions in structural biology. *Proc. Natl. Acad. Sci. U.S.A.* 96, 9459–9464.
- (49) Ragsdale, D. S., McPhee, J. C., Scheuer, T., and Catterall, W. A. (1994) Molecular determinants of state-dependent block of Na<sup>+</sup> channels by local anesthetics. *Science* 265, 1724–1728.
- (50) Decher, N., Pirard, B., Bundis, F., Peukert, S., Baringhaus, K. H., Busch, A. E., Steinmeyer, K., and Sanguinetti, M. C. (2004) Molecular basis for Kv1.5 channel block: Conservation of drug binding sites among voltage-gated K<sup>+</sup> channels. *J. Biol. Chem.* 279, 394–400.
- (51) Trellakis, S., Benzenberg, D., Urban, B. W., and Friederich, P. (2006) Differential lidocaine sensitivity of human voltage-gated potassium channels relevant to the auditory system. *Otology & Neurotology* 27, 117–123.
- (52) Becker, D. E., and Reed, K. L. (2006) Essentials of local anesthetic pharmacology. *Anesth. Prog.* 53, 98–109.
- (53) Quan, C., Mok, W. M., and Wang, G. K. (1996) Use-dependent inhibition of Na<sup>+</sup> currents by benzocaine homologs. *Biophys. J.* 70, 194–201.
- (54) Wang, G. K., Quan, C., and Wang, S. (1998) A common local anesthetic receptor for benzocaine and etidocaine in voltage-gated  $\mu$ 1 Na<sup>+</sup> channels. *Pfluegers Arch.* 435, 293–302.
- (55) Bokesch, P. M., Raymond, S. A., and Strichartz, G. R. (1987) Dependence of lidocaine potency on pH and P<sub>CO<sub>2</sub></sub>. *Anesth. Analg. (Hagerstown, MD, U.S.)* 66, 9–17.
- (56) Hargreaves, K. M., and Keiser, K. (2002) Local anesthetic failure in endodontics: Mechanisms and management. *Endodontic Topics* 1, 26–39.
- (57) Ueno, T., Tsuchiya, H., Mizogami, M., and Takakura, K. (2008) Local anesthetic failure associated with inflammation: Verification of the acidosis mechanism and the hypothetical participation of inflammatory peroxynitrite. *J. Inflammation Res.* 1, 41–48.
- (58) Tsuchiya, H., Mizogami, M., Ueno, T., and Takakura, K. (2007) Interaction of local anaesthetics with lipid membranes under inflammatory acidic conditions. *Inflammopharmacology* 15, 164–170.
- (59) Bodendiek, S. B., Rubinos, C., Trelles, M. P., Coleman, N., Jenkins, D. P., Wulff, H., and Srinivas, M. (2012) Triarylmethanes, a new class of Cx50 inhibitors. *Front. Pharmacol.* 3, 106.